Impedance-based Sensitivity Analysis of Dual Active Bridge DC-DC Converter

Jiajun Yang, Giampaolo Buticchi, Hao Yan, Chunyang Gu, He Zhang, Pat Wheeler
Key Laboratory of More Electric Aircraft Technology of Zhejiang Province
University of Nottingham Ningbo China
Ningbo, China
jiajun_yang@outlook.com

***Abstract*—The sensitivity analysis of a circuit reflects the robustness of this circuit to the relevant parameters. This paper investigates the sensitivity of input impedance of DAB converter, which is widely adopted in solid-state transformer (SST) and dc microgrid on more electric aircraft (MEA). In this paper, an improved impedance-based small-signal averaged model is developed to carry out the sensitivity analysis. Bode plots will be used as main analysis tool. The small signal model is compared to a complete switching model to confirm the validity of the proposed approach.**

Keywords—Dual active bridge dc-dc converter, impedance-based small-signal averaged model, sensitivity analysis, input impedance.

I. INTRODUCTION

Compared to conventional aircraft and all electric aircraft (AEA), the concept of more electric aircraft (MEA) is more preferred by aerospace industries as a step-wise approach, in order to limit risks and gaining experience [1]. During the last several decades, significant progress has been made to move toward MEA. Many onboard hydraulic, mechanical and pneumatic devices have been partially or fully replaced with electrical devices [2]. Also, the shortage of conventional energies accelerates the irresistible process of electrifying onboard devices. For example, in electrification of hydraulic systems, it is stated in [2]-[4] that the conventional hydraulic actuator is supposed to be replaced with electro-hydraulic actuator (EHA) or electromechanical actuator (EMA) because of its bulky size, easily jamming and leaking. Both EHA and EMA are controlled by solid state power electronics and variable speed motor drives. It is also reported in [3] that the EHA system has been adopted in the newest civilian aircrafts Boeing 787 and Airbus 380, to replace the conventional hydraulic actuator. This leads to a more flexible and leakless framework. However, to achieve a completely jamming free and leaking free actuator system with high reliability and safety, it is envisaged to use EMA system to get rid of hydraulic power entirely in future.

Consequently, by introducing more electrical devices into aircraft, the onboard electrical power generation increases while the challenges in designing an efficient and secure electrical power distribution system arise [3]. The onboard electrical power distribution system can be regarded as a microgrid since the aircraft is an isolated system with generators and loads [4]. Several different voltage standards applied for electrical system on large civilian aircraft are listed in [5], containing both ac and dc levels. Compared with ac microgrid, dc microgrid has the advantage of featuring fewer components due to reduced conversion stages, resulting in lower possibility to failures and lower weight [4]. A conventional dc microgrid contains multiple dc-dc converters to interface multiple sources and loads. Although this pattern allows power flow simultaneously, it is too complex and expensive because of more conversion stages and communication devices between converters [6]. To solve this problem, multiport dc-dc converter is proposed in which all ports are bidirectional, to reduce the number of conversion stages. Furthermore, voltage droop control as a kind of decentralized control methods, is introduced in [4] to achieve power sharing between converters with different sources/generators by establishing a virtual resistor, eliminating the communication devices.

When it comes to dc-dc converters applied to the microgrid on MEA, the converters must have the characteristic of galvanic isolation for safety purposes [7]. Hence, a converter containing a dc-ac inverter, a main transformer and a diode bridge rectifier can be the basic structure to achieve galvanic isolation. By applying the phase-shift modulation to inverter part, high efficiency unidirectional power flowing can be achieved. Furthermore, the diodes in rectifier also can be replaced with switches to realize bidirectional power flowing and enable both boost and buck modes. Among variety of bidirectional power flowing converters, dual active bridge (DAB) converter is the most classical topology which has drawn many researchers' attention in aerospace applications by its features in terms of high-power density, high efficiency and bidirectional power flow [8]. Although DAB converter is widely used in both researches and industrial applications, the stability of it needs to be thoroughly assessed when it is adopted in the microgrid for avionic use. In this paper, Section II gives the structure and operation principle of DAB converter. Section III presents an improved impedance-based small-signal model of DAB converter and also sensitivity analysis of the model by changing parameters of the circuit. Section IV provides specifications for DAB converter. Section V investigates the sensitivity of input impedance of DAB converter by changing specification parameters. Section VI presents the simulation results of impedance-based model and switching model. Section VII draws a conclusion and summarizes the contribution of this work.

II. DUAL ACTIVE BRIDGE CONVERTERS

The simplified structure of DAB converter is presented in Fig. 1.

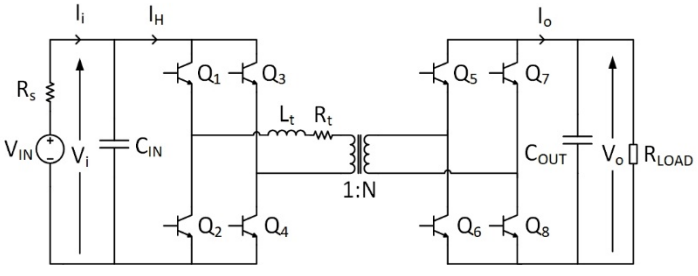

Fig. 1. Simplified schematic of DAB converter

By employing phase-shift modulation to full bridges on both sides, the conversion between dc power and ac power is realized. In addition, the phase shift between switching signals of both sides determine the direction of power flowing. When the primary side bridge leads the secondary side bridge, the power will flow to load from supply. Conversely, when the primary side bridge lags, the power will flow back to supply from load. Fig. 2 shows the ideal operating waveforms of the DAB converter at the primary side bridge leading mode, in which power is flowing from source to load. The idealized output power equation of DAB converter at steady state is derived as

$$P_o = I_H V_i = I_o V_o = \frac{V_i V_o}{2Nf_s L_t} d(1-|d|) \tag{2.1}$$

where V_i is the input voltage, I_H is the input current, V_o is the output voltage, I_o is the output current. N is the turn ratio of the HF transformer, f_s is the switching frequency, L_t is the leakage inductance of the HF transformer, d is phase shift ratio equal to $\frac{\varphi}{\pi}$. By controlling the phase shift, the transferred power can be controlled.

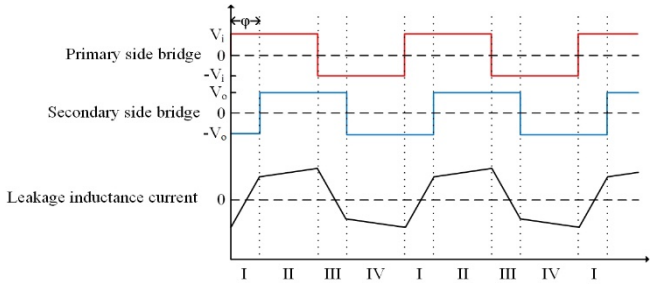

Fig. 2. Operating waveforms of DAB converter

III. Impedance-based small-signal model of DAB converter

Generally, state-space equation averaging technique and circuit averaging technique are often used to obtain the small-signal averaged model of a converter circuit [9]. However, it is less easy when they are applied to converters with more complex structure such as DAB converter. So far, several kinds of models of DAB converter has been proposed by researchers in [10]-[12]. In this section, an alternative method is proposed to obtain the small-signal averaged model of DAB converter, which is to model the input impedance by using the small-signal equations derived from the power equation of DAB converter. By using Equation (2.1), the input current I_H and output current I_o can be obtained as

$$I_H = \frac{V_o}{2Nf_s L_t} d(1-|d|) \tag{3.1}$$

$$I_o = \frac{V_i}{2Nf_s L_t} d(1-|d|) \tag{3.2}$$

By deriving Equation (3.1) and Equation (3.2) partially to V_i, V_o and d, the small-signal equations are shown as

$$\hat{I}_H = \frac{1}{2Nf_s L_t}[\hat{d}(1-|2\bar{d}|)\bar{V}_o + \hat{V}_o(1-|\bar{d}|)\bar{d}] \tag{3.3}$$

$$\hat{I}_o = \frac{1}{2Nf_s L_t}[\hat{d}(1-|2\bar{d}|)\bar{V}_i + \hat{V}_i(1-|\bar{d}|)\bar{d}] \tag{3.4}$$

In Equation (3.3) and (3.4), 'triangles' are used to indicate small signals and 'bars' are used to indicate large signals. By applying KCL with these two small-signal equations, a block scheme can be worked out in Fig. 3.

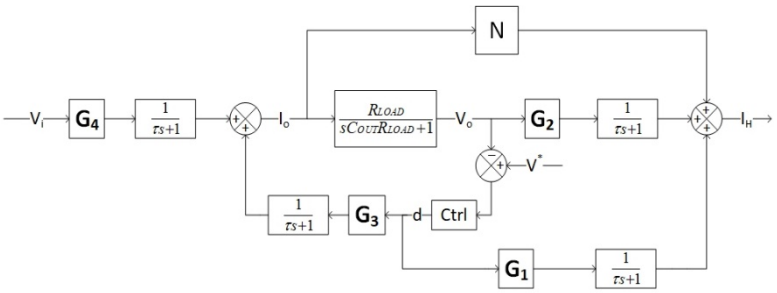

Fig. 3. Block scheme of DAB converter based on small-signal equations

To depict the block scheme in a simpler way, the gain between small-signal variables are represented in blocks G_1, G_2, G_3 and G_4. The specific equations of these four blocks are expounded as

$$G_1 = \frac{1}{2Nf_s L_t}(1-|2\bar{d}|)\bar{V}_o,\ G_2 = \frac{1}{2Nf_s L_t}(1-|\bar{d}|)\bar{d},$$
$$G_3 = \frac{1}{2Nf_s L_t}(1-|2\bar{d}|)\bar{V}_i,\ G_4 = \frac{1}{2Nf_s L_t}(1-|\bar{d}|)\bar{d} \tag{3.5}$$

By observing these four gains, it is easy to find that G_2 and G_4 are same, meantime G_1 is proportional to G_3. A similar block scheme based on small-signal equations was obtained in [13]. However, it misses the consideration of time delay. In Fig. 3 the function '$\frac{1}{\tau s+1}$' is added as a first-order time delay function. The symbol 'τ' is the time constant to represent the time delay from the moment when switches are operated to the moment the output is rectified. In this case the time delay is assumed to be one switching period. In addition, in Fig. 3 the input current I_H and output current I_o are also connected by the gain block N which is the turn ratio of transformer. According to this block scheme, the transfer function of input admittance can be figured out as

$$Y_i(s) = \frac{I_H(s)}{V_i(s)} = \frac{G_4 T_D N(1+sR_{LOAD}C_{OUT}) + G_2 G_4 {T_D}^2 R_{LOAD} - G_1 G_4 {T_D}^2 R_{LOAD} Ctrl}{1+sR_{LOAD}C_{OUT} + G_3 Ctrl T_D R_{LOAD}} \tag{3.6}$$

where 'Ctrl' is the transfer function of controller, T_D represents the first-order time delay function $\frac{1}{\tau s+1}$, G_1, G_2, G_3 and G_4 are the gains. Based on that, the input impedance Z_i including the input capacitor C_{IN} can be calculated in a more detailed form as

$$Z_i(s) = \frac{1}{Y_i + sC_{IN}} = \frac{1+sR_{LOAD}C_{OUT} + G_3 Ctrl T_D R_{LOAD}}{G_4 T_D N(1+sR_{LOAD}C_{OUT}) + G_2 G_4 {T_D}^2 R_{LOAD} - G_1 G_4 {T_D}^2 R_{LOAD} Ctrl + sC_{IN}(1+sR_{LOAD}C_{OUT} + G_3 Ctrl T_D R_{LOAD})} \tag{3.7}$$

IV. Specifications

Before analyzing the sensitivity of input impedance of DAB converter, specifications should be given. Then the sensitivity can be analyzed by changing the parameters in a reasonable range. The specifications are shown in Table. 1. In this case, the controller is determined to be the PI (proportional + integral) type because PI control has not only fast dynamic response but also good immunization to noise.

Parameter	Value	Parameter	Value
V_i	270V	C_{IN}	5 mF
V_o	28V	C_{OUT}	5 mF
N	28/270	K_p	0.001
L_t	0.2 mH	K_i	10
f_s	50 kHz	d	0→0.2(default)
R_s	1 ohm	R_{LOAD}	1.344 ohm→∞
R_t	0.04 ohm	d and R_{LOAD} are dependent to each other	

Table. 1. Specifications of DAB converter and PI controller

V. Sensitivity Analysis

To analyze the sensitivity of input impedance, several important parameters are supposed to be changed: the phase shift ratio (the default value is 0.2), the load, the output capacitor, the parameters of controller, the type of controller and the switching frequency. To observe the change of input impedance in a more intuitional way, Matlab is used to plot the Bode diagram of input impedance by changing parameters. The sensitivity of input impedance of DAB converter to parameters plotted in Fig. 4.

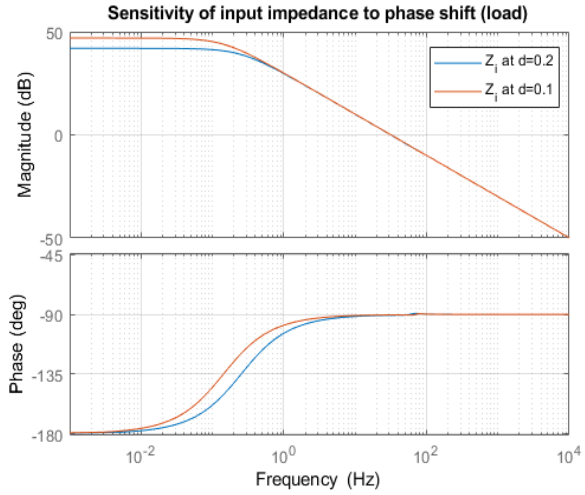

(a) The phase shift ratio d = 0.2 → 0.1 (R_{LOAD} = 1.344 ohm→ 2.39ohm)

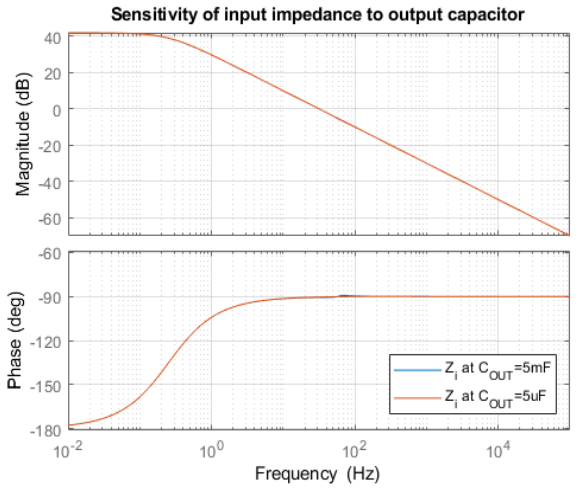

(b) The output capacitor C_{OUT} = 5m F → 5μ F

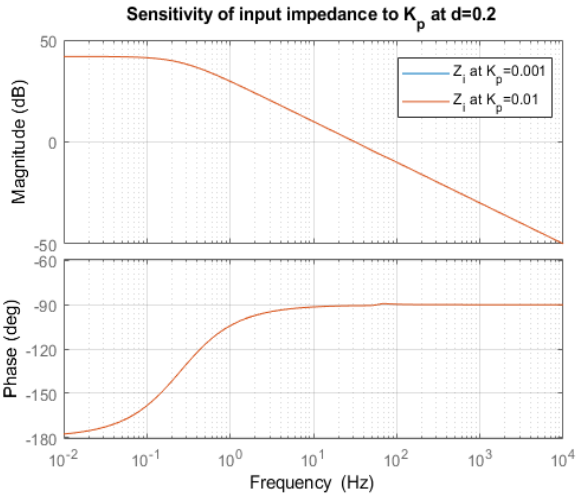

(c) The parameter of controller K_p = 0.001 → 0.01

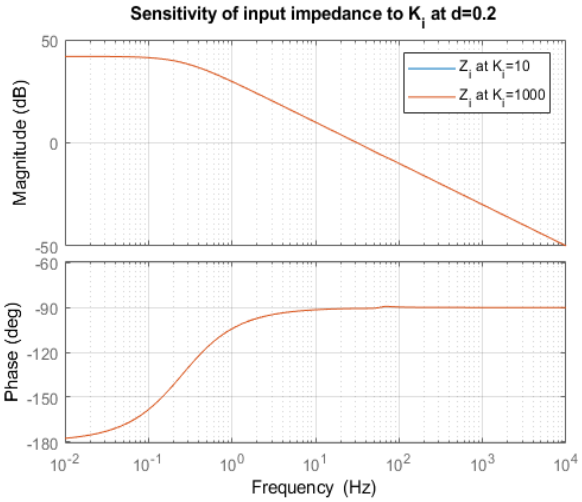

(d) The parameter of controller K_i = 10 → 1000

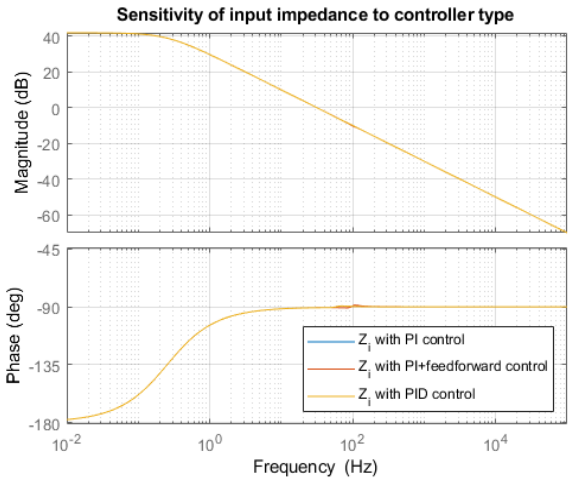

(e) The type of controller PI → PI + feedforward & PID

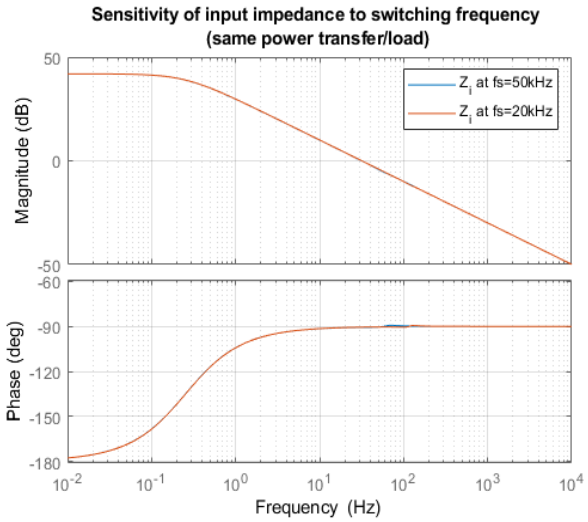

(f) The switching frequency fs = 50kHz → 20kHz
(Phase shift is adjusted to keep same power transfer/load)

Fig. 4. Sensitivity of input impedance of DAB converter to parameters

In Fig. 4, six bode diagrams (a), (b), (c), (d), (e) and (f) show the curves of input impedance of DAB converter according to different parameters of circuit. All parameters are changed in a proper range to keep the whole system still stable. In (a), the input impedance changes slightly in both magnitude and phase when the phase shift ratio d changes (load also changes because the power changes). In (b), (c), (d), (e) and (f) the input impedance almost keeps same when the output capacitor, the parameters of controller, the type of controller and the switching frequency changes. This means the sensitivity of input impedance to circuit parameters are very low if the transferred power is constant. In addition, it can be observed that the input impedance performs as a constant power load which has negative incremental impedance characteristic with phase close to -180° at low frequencies, while the input impedance starts to perform as a capacitor with phase close to -90° at higher frequencies.

VI. Validation

To validate the small-signal model stated in Section III, the method is adding an external sinusoidal current into input current and then observe the changes in input voltage. Two simulation models are built by PLECS: 1) A switching model and 2) An impedance-based model. In the switching model, all components are ideal, and they are connected like the schematic shown Fig. 1, the value of them are same as the parameters shown in Table. 1. The purpose of impedance-based model is to obtain the same results by using transfer function. By comparing the results of these two models, the small-signal model can be verified.

In the step of validation, sinusoidal ac current with amplitude of 10A and various frequencies is injected at t=0.1s. The phase shift ratio d is adjusted to be 0.2. By comparing the input voltage of both two simulation models, the transfer function of input impedance can be verified. Moreover, the characteristic of input impedance can be figured out by observing the variations of both input current and input voltage, and then be verified with the bode diagrams in Fig. 4. The input voltage and input current waveforms of two simulation models injected by current with different frequencies are shown in Fig. 5.

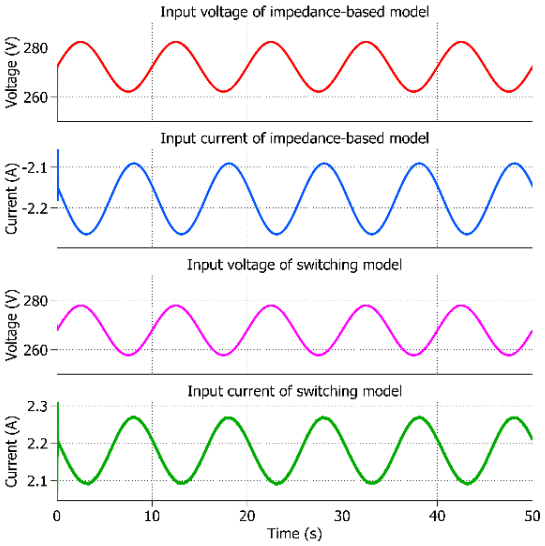

(a) Waveforms with injected current frequency of 0.1Hz

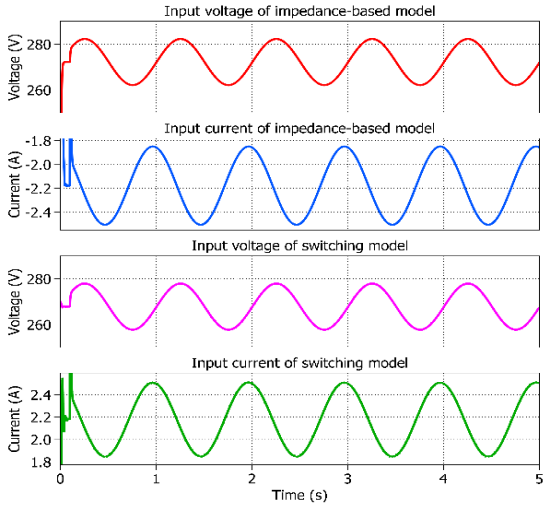

(b) Waveforms with injected current frequency of 1Hz

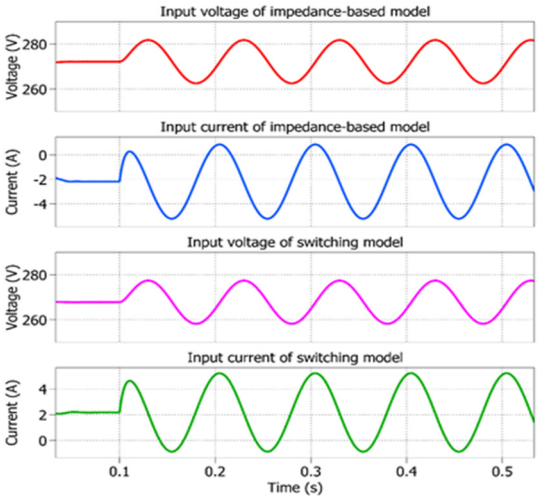

(c) Waveforms with injected current frequency of 10Hz

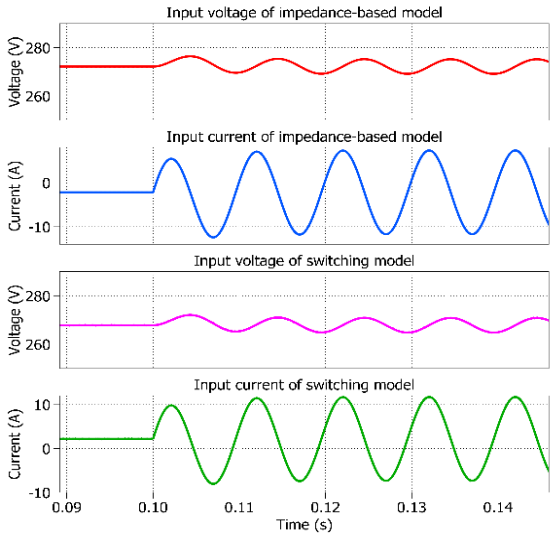

(d) Waveforms with injected current frequency of 100Hz

Fig. 5. Input voltage and input current waveforms with different injected current frequencies (0.1Hz, 1Hz, 10Hz and 100Hz)

The high consistency of input voltage in both two simulation models proves that the transfer function of input impedance is correct. In addition, it is worth to mention that the input current of the impedance-based circuit model is negative, indicating that the input current flowing to source. It is reasonable because the transfer function of input impedance must have phase close to -180° at low frequencies to make the converter stable. Besides, the characteristic of input impedance can be clarified by calculating the ratio of the peak-to-peak value of input voltage to input current in fluctuating state and then verifying with the bode diagram in Fig. 4. The approximate ratios of four figures in Fig. 5 are: (a) 41.3dB at 0.1Hz, (b) 29.7dB at 1Hz, (c) 10.1dB at 10Hz, (d) -10.1dB at 100Hz. Hence, all of them are almost settled in the curve of input impedance in Fig. 4, proving that the input impedance of DAB converter performs as a constant power load at low frequencies while it performs as a capacitor at high frequencies.

ACKNOWLEDGMENT

This work was supported by the Ningbo Science & Technology Bureau, China under Grant 2014A35007 and Grant 2017D10031, the Ningbo 3315 Innovation Team Scheme under Grant 2018A-08-C, and the Zhejiang Key Laboratory Programme under Grant 2019E10018.

VII. CONCLUSION

An improved impedance-based small-signal model of phase-shift controlled DAB converter is proposed in this paper. It uses small-signal equations derived from the power equation to obtain an appropriate block scheme including time delay, and then the transfer function of input impedance is worked out. The Bode diagram of input impedance is plotted by using Matlab. In addition, the sensitivity of input impedance to the phase shift ratio (load), the output capacitor, the parameters of controller, the type of controller and the switching frequency is analyzed. It shows that the sensitivity of input impedance to these important circuit parameters is very low if the transferred power is constant. Besides, to validate whether the transfer function is correct, PLECS is used to create a switching model and impedance-based model injected by current with different frequencies. The input voltage of these two models is nearly consistent, proving that the transfer function is correct. Moreover, the characteristic of input impedance is verified by calculating the ratio of the peak-to-peak value of input voltage to input current in fluctuating state. As a result, the input impedance behaves as a constant power load at low frequencies and behaves as a capacitor at high frequencies.

REFERENCES

[1] R. I. Jones, “The More Electric Aircraft: the past and the future?,” in IEE Colloquium on Electrical Machines and Systems for the More Electric Aircraft (Ref. No. 1999/180), 1999, pp. 1/1-1/4.

[2] B. Sarlioglu and C. T. Morris, “More Electric Aircraft: Review, Challenges, and Opportunities for Commercial Transport Aircraft,” IEEE Transactions on Transportation Electrification, vol. 1, no. 1, pp. 54–64, Jun. 2015.

[3] J. A. Rosero, J. A. Ortega, E. Aldabas, and L. Romeral, “Moving towards a more electric aircraft,” IEEE Aerospace and Electronic Systems Magazine, vol. 22, no. 3, pp. 3–9, Mar. 2007.

[4] G. Buticchi, L. Costa, and M. Liserre, “Improving System Efficiency for the More Electric Aircraft: A Look at dc\/dc Converters for the Avionic Onboard dc Microgrid,” IEEE Industrial Electronics Magazine, vol. 11, no. 3, pp. 26–36, Sep. 2017.

[5] P. Wheeler and S. Bozhko, “The More Electric Aircraft: Technology and challenges.” IEEE Electrification Magazine, vol. 2, no. 4, pp. 6–12, Dec. 2014.

[6] H. Tao, A. Kotsopoulos, J. L. Duarte, and M. A. M. Hendrix, “Family of multiport bidirectional DC-DC converters,” IEE Proceedings - Electric Power Applications, vol. 153, no. 3, pp. 451–458, May 2006.

[7] G. Buticchi, S. Bozhko, M. Liserre, P. Wheeler, and K. Al-Haddad, “On-Board Microgrids for the More Electric Aircraft—Technology Review,” IEEE Transactions on Industrial Electronics, vol. 66, no. 7, pp. 5588–5599, Jul. 2019.

[8] M. N. Kheraluwala, R. W. Gascoigne, D. M. Divan, and E. D. Baumann, “Performance characterization of a high-power dual active bridge DC-to-DC converter,” IEEE Transactions on Industry Applications, vol. 28, no. 6, pp. 1294–1301, Nov. 1992.

[9] R. W. Erikson and D. Maksimovic, Fundamentals of power electronics, 2nd ed. Norwell, Mass.: Kluwer Academic, 2001.

[10] H. Qin and J. W. Kimball, “Generalized Average Modeling of Dual Active Bridge DC–DC Converter,” IEEE Transactions on Power Electronics, vol. 27, no. 4, pp. 2078–2084, Apr. 2012.

[11] J. A. Mueller and J. W. Kimball, “An Improved Generalized Average Model of DC–DC Dual Active Bridge Converters,” IEEE Transactions on Power Electronics, vol. 33, no. 11, pp. 9975–9988, Nov. 2018.

[12] J. A. Mueller and J. W. Kimball, “Model-based determination of closed-loop input impedance for dual active bridge converters,” in 2017 IEEE Applied Power Electronics Conference and Exposition (APEC), 2017, pp. 1039–1046.

[13] M. Khazraei, V. A. K. Prabhala, R. Ahmadi, and M. Ferdowsi, “Solid-state transformer stability and control considerations,” in 2014 IEEE Applied Power Electronics Conference and Exposition - APEC 2014, 2014, pp. 2237–2244.